

# Time-Dependent Earthquake Probability Computations and Fault Interaction Effects in Zagros, Iran

Hamid Zafarani<sup>1\*</sup> and Samaneh Kazem<sup>2</sup>

1. Associate Professor, Seismology Research Centre, International Institute of Earthquake Engineering and Seismology (IIEES), Tehran, Iran,

\*Corresponding Author; email: h.zafarani@iiees.ac.ir

2. M.Sc. Graduate, AleTaha Institute of Higher Education, Tehran, Iran

Received: 10/12/2018

Accepted: 09/05/2021

## ABSTRACT

When a relatively strong earthquake occurs, it changes the conditions for failure in its proximity and alters the occurrence probability for future events. In this study, the occurrence probability of future earthquakes with magnitudes  $M_w \geq 5.8$  on the basis of Brownian passage-time (BPT) and Weibull Time-dependent models is calculated for the next 10, 30 and 50 years in the Zagros region. According to the method used in recent years, initially, the Coulomb stress changes caused by earthquakes interaction is computed on each fault. Then, the impact of this stress change on the occurrence probability of next characteristic earthquakes is calculated, taking into account both permanent (clock advance) and transient (rate-and-state) effects of stress changes. We concentrated on the long term slip rate uncertainties by generating 1000 random numbers using the Monte Carlo technique. We find that earthquake interaction effects in this region are small. Thus, permanent and transient effects of stress change do not affect the calculated probabilities very much. The maximum probability is related to the Kazerun fault that shows the high seismic activity of this fault.

### Keywords:

Coulomb stress;  
Time-dependent Model;  
Probability; Weibull;  
Brownian passage-time

## 1. Introduction

Earthquakes are usually triggered when the rock overlying fault lines, breaks and suddenly releases a significant amount of energy. Large Earthquakes change the average shear and normal stress of the slipping faults, and consequently change the seismicity rate and the earthquake occurrence probability of faults or fault segments provided that large shocks occur repeatedly at approximately regular intervals. In recent years, the interaction of faults is calculated by Coulomb static stress change, also known as the Coulomb failure function. The stress change can be positive (stress increment) or negative (stress reduction). Positive Coulomb stress changes amplify the background seismicity, and as a result, in areas of high background activity, small stress changes would

cause large changes in the seismicity rate [1].

Fault interactions may accelerate or delay the fault rupture, or trigger an earthquake momentarily [2]. Since the occurrence of a characteristic earthquake may alter the occurrence probability of the future events in the region, consideration of fault interactions based on physical models and combining it with renewal models such as the Brownian passage time (BPT) and Weibull would lead us to achieve more precise results.

In recent years, several studies were conducted in this regard [3]. In order to improve the results of earthquake occurrence probability, the effect of Coulomb stress change caused by interactions should be considered in probabilistic models. In the renewal

processes, also called time-dependent models, the conditional probability of next eventual large earthquake alters with time, so that the probability is low shortly after the last one, but then raises with time. Time-dependent models were used to survey shocks on single faults [4-5] or in seismic sources including the main fault where the characteristic earthquake is generated as well as other smaller faults, where smaller main shocks also occur [6-7].

The Zagros fold-thrust belt, extending from eastern Turkey to the Strait of Hormoz, 250-400 km wide, is one of the most seismically active belts in Asia. The Zagros fold and thrust belt formed in the foreland of the collision between the Arabian Plate and the Eurasian Plate. Due to the importance of this zone, the Zagros region in Iran included in the rectangle of coordinates 27-31.2°N and 49.6-53.4°E is selected as the study area (Figure 1). The occurrence probability of earthquakes with  $M_w \geq 5.8$  with regard to both transient and permanent effects of Coulomb stress change is computed for periods of 10, 30 and 50 years. The BPT and Weibull distributions are used to calculate the conditional probabilities of characteristic earthquakes. Modeling of earthquakes and receiver faults such as Kazerun,

Sabzpushan, Qir, Karebas and parts of MFF (Zagros Mountain Front fault) and ZFF (Zagros Foredeep fault) and stress computation is conducted by using Coulomb 3.3 software. The purpose of the present study is to estimate the probability of occurrence of an earthquake with  $M_w \geq 5.8$  taking into account the uncertainties involved in slip rate and recurrence time of earthquakes, and to identify areas with high probability of earthquake occurrence in the Zagros region.

## 2. Method

Estimation of long-term probabilities of occurrence of earthquakes of specific size in a given time interval is the primary goal in seismic hazard assessment. Generally, two types of models have been used to calculate the conditional probability of the next large earthquake: Time-independent Poisson model and renewal model. The Poissonian hypothesis is memoryless. Scilicet this model assumes that future earthquake is equally plausible immediately after the past one as it is much later and the probability of occurrence of an earthquake in a specific period does not depend on the time elapsed after the last earthquake. An alternative is to use time-dependent

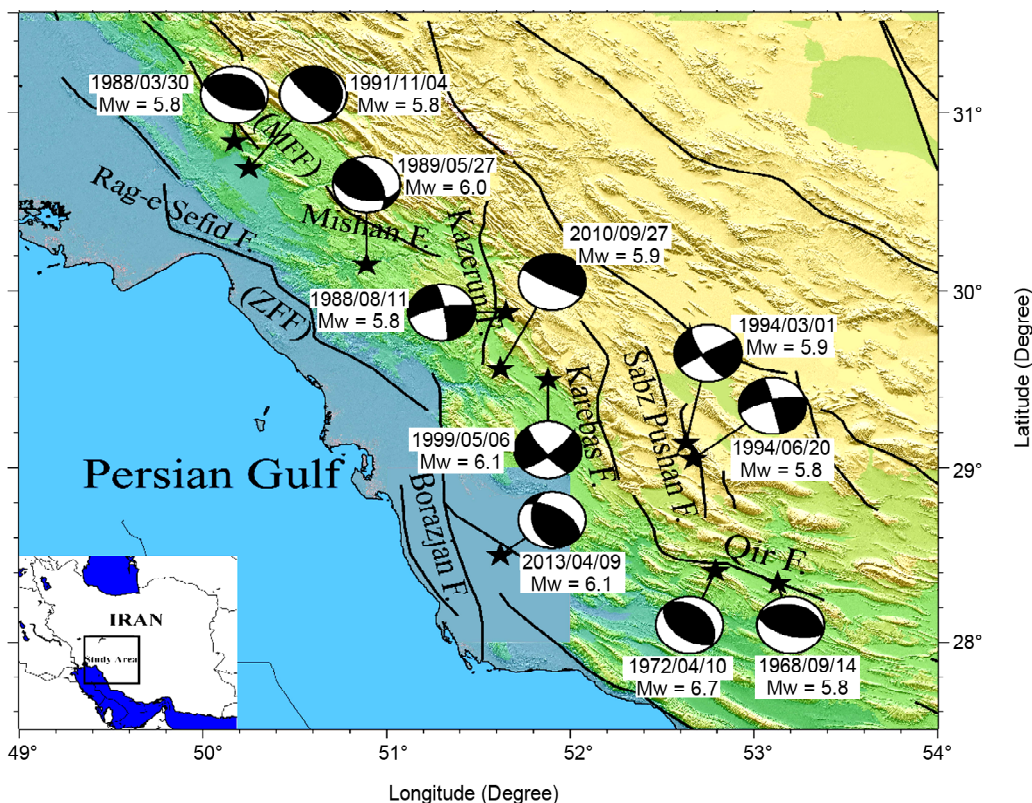


**Figure 1.** Map of the study area in the Zagros region limited by the rectangle of coordinates 27-31.2° N° and 49.6-53.4° E°, where active faulting and fault-plane solutions of characteristic earthquakes with  $M_w \geq 5.8$  during 1964-2016 are depicted.

models in which some probability distributions, describe the elapsed time between large earthquakes [8-9]. Renewal models describe the occurrence of earthquakes as sequence of events with independent and identically distributed inter-event times [10-11]. Various time-dependent seismic hazard analysis schemes differ mainly in the statistical distribution of time interval between consecutive events of each fault. Several models are proposed for the probability density function (pdf) of inter-event time periods such as the Normal, Gamma; Lognormal, Weibull and BPT distributions. The latter sufficiently expresses the earthquake recurrence time distribution and was proposed to characterize the probability distribution of inter-event times [12]. In the BPT model, the value of the stress is raised linearly from a basis state to a stress threshold. The BPT hazard rate increases from zero to a finite asymptotic level unto the mean recurrence time and then decreases toward a non-zero constant asymptote [12]. The pdf of BPT distribution for recurrence time based on the mean inter-event time  $T_r$ , and the elapsed time from the occurrence of the last characteristic earthquake  $t$  is defined as follows:

$$f(t, T_r, \alpha) = \left( \frac{T_r}{2\pi\alpha^2 t^3} \right)^{\frac{1}{2}} \exp \left\{ -\frac{(t - T_r)^2}{2T_r \alpha^2 t} \right\} \quad (1)$$

where  $\alpha$ , the coefficient of variation of the distribution, also called the aperiodicity parameter, is defined as the ratio of the standard deviation  $\sigma_T$  to the average inter-event time  $\bar{T}$ . For clustered earthquakes occurrence,  $\alpha$  must be greater than 1. For a completely accidental seismicity (Poisson process) and absolutely cyclic events, this factor should be equal to 1 and 0, respectively. In this study, we considered  $\alpha$  values in the range of 0.5-0.75 for individual faults [13].

The Weibull distribution that is widely used in engineering applications nowadays follows fracture mechanics and statistical physics [14-15]. The Weibull hazard-rate functions start from zero at  $t=0$  and then increase relatively steeply [12]. In addition, this distribution is often used as probability density function of inter-event times [16]. For this model, in addition to the parameters mentioned in the previous section, the shape parameter of the distribution  $\gamma$  that is equivalent to the inverse of the coefficient of variation is needed. The Weibull distribution [14] is

expressed according to Equation (2):

$$f(t, T_r, \gamma) = \frac{\gamma}{T_r} \left( \frac{t}{T_r} \right)^{\gamma-1} \exp \left\{ -\left( \frac{t}{T_r} \right)^\gamma \right\} \quad (2)$$

The hazard function,  $h(t)$ , which is the probability that an earthquake will occur at time  $t$  provided that it has not previously occurred, is given by:

$$h(t) = \frac{f(t)}{1 - F(t)} \quad (3)$$

where  $f(t)$  and  $F(t)$  are probability density function and cumulative density function of the inter-event times, respectively. The conditional time-dependent probability that an earthquake will occur between times  $t$  and  $t + \Delta t$ , provided that the earthquake has not been occurred prior to time  $t$ , can be written as:

$$pr[t < T \leq t + \Delta t | T > t] = \frac{pr[t < T \leq t + \Delta t]}{pr[t < T]} \quad (4)$$

In order to assess how a fault or the rupture plane of target event has been brought closer or further from the failure due to preceding earthquakes, we use the Coulomb failure function:

$$\Delta CFF = \Delta\tau + \mu' \Delta\sigma_n \quad (5)$$

where  $\Delta CFF$ ,  $\Delta\tau$  and  $\Delta\sigma_n$  are the changes in Coulomb stress, shear stress and normal stress of the causative fault plane, respectively. Normal stress is positive if the fault is unclamped. The  $\mu'$  represents the apparent coefficient of friction that includes the unknown effect of pore pressure change and is believed to range between 0 and 0.75 [17]. This coefficient, based on the Skempton coefficient  $B$  and the friction coefficient  $\mu$ , is expressed as:

$$\mu' = \mu(1 - B) \quad (6)$$

When  $\mu'$  is high, the pore pressure does not influence the normal stress. The rock is so saturated when  $\mu' = 0$  so that the pore pressure demolishes the influence of the normal stress [18]. We set  $\mu' = 0.4$ , which is closer to the laboratory amounts of the major faults frictions ( $\mu = 0.75$ ) [19]. The Skempton coefficient varies between 0 and 1 [20]. In the Coulomb criterion, the failure occurs on a plane where the coulomb stress  $\sigma_f$  exceeds a specific maximum value.

Combination of the calculated Coulomb stress changes  $\Delta CFF$  with earthquake probability computations for the next characteristic event requires the use of stress change as an advance or delay in the earthquake cycle. Two approaches are considered to assess the permanent effect of Coulomb stress change on the probability of characteristic earthquake [21]. The first approach advances the elapsed time by modifying the time elapsed after the last event from  $t$  to  $t'$ :

$$t' = t + \frac{\Delta CFF}{\dot{\tau}} \quad (7)$$

where  $\dot{\tau}$  is the tectonic stressing rate. The second method decreases the expected mean recurrence time from  $T_r$  to  $T'_r$ :

$$T'_r = T_r - \frac{\Delta CFF}{\dot{\tau}} \quad (8)$$

In this study, assuming that both techniques present the same conclusions, the first method is selected. The transient effects are derived from the rate-and-state model for earthquake nucleation [22]. The expected seismicity rate  $R(t)$  as a function of time,  $t$ , after a stress perturbation, derived from Dieterich's constitutive friction law [22], is given by:

$$R(t) = \frac{R_0}{\left[ \exp\left(\frac{-\Delta CFF}{A\sigma}\right) - 1 \right] \exp\left(-\frac{t}{t_a}\right) + 1} \quad (9)$$

where  $R_0$  is the seismicity rate prior to change of stress,  $A\sigma$  is the combination of fault constitutive constant and normal stress, in other words  $A\sigma$

explains the immediate response of friction to a step change in the slip speed [23],  $t_a$  is the characteristic relaxation time for the perturbation (also referred as observed aftershock duration). Also, it has been proposed for nucleation sites that are close to rupture, indicates the time that would be elapsed until the seismicity rate to reach its initial value before the earthquake occurrence [22, 24], that is:

$$t_a = \frac{A\sigma}{\dot{\tau}} \quad (10)$$

where  $\dot{\tau}$  is the tectonic stressing rate. Since,  $t_a$  and  $A\sigma$  are unknown for Zagros, we set  $t_a = 1.4$  year, the value is derived from window algorithm for aftershocks [25], and then by substituting  $\dot{\tau}$  and  $t_a$  in the above equation, we obtained  $A\sigma$  parameter. Therefore, the occurrence probability of an earthquake taking into account the transient effects is computed by:

$$p = 1 - \exp(-N) = 1 - \exp\left(-\int_t^{t+\Delta t} R(t) dt\right) \quad (11)$$

where  $N$  is the expected number of earthquakes in the time interval  $t$  and  $t + \Delta t$ .

### 3. Data and Results

Computation of Coulomb stress change of receiver fault caused by the characteristic events requires information about the date of the events with  $M_w \geq 5.8$ , the magnitude and depth, hypocentral coordinates, faulting type and fault plane solutions. Table (1) contains the essential information needed for modeling major faults and

**Table 1.** Source Parameters of the  $M_w \geq 5.8$  earthquakes that occurred in the area of Zagros during 1964-2016.

#	Source Name	Date			$M_w$	Location		Faulting Type	Depth (km)	Fault Plane Solution			Ref.
		Year	Month	Day		Longitude (E)	Latitude (N)			Strike (°)	Dip. (°)	Rake (°)	
1	Kazerun	1988	8	11	5.8	51.65	29.88	SS	9	350	82	-166	[26, 27]
2	Kazerun	2010	9	27	5.9	51.62	29.56	SS	17.1	119	85	89	[28]
3	-	2013	4	9	6.1	51.62	28.51	-	9	164	42	119	[29]
4	Sabz Pushan	1994	3	1	5.9	52.63	29.14	SS	13	149	75	177	[31]
5	Sabz Pushan	1994	6	20	5.8	52.67	29.05	SS	9	255	74	-3	30, 31
6	Karebas	1999	5	6	6.1	51.88	29.50	SS	7	142	78	-167	[31]
7	Qir	1968	9	14	5.8	53.18	28.34	T	7	288	30	90	[31, 32]
8	Qir	1972	4	10	6.7	52.79	28.41	T	10	322	40	98	[27, 31]
9	MFF	1988	3	30	5.8	50.18	30.85	T	15	296	32	90	[28, 31]
10	MFF	1991	11	4	5.8	50.25	30.69	T	5	135	80	78	[31]
11	ZFF	1989	5	27	6	50.89	30.15	T	15	332	57	122	[28, 31]

SS: Strike Slip

T: Thrust

earthquakes in the study area.

As, for all the considered faults in this study, fault shape and slip heterogeneity are both uncertain, it is assumed that all faults are rectangular and have uniform slip distribution. In order to calculate the length and width of rupture, Wells and Copper-smith [33] empirical relationships among magnitude,

rupture length and rupture width is used.

The fault depth required for the calculation of stress change is assumed to be equal to 10 km. The Coulomb stress change due to events with  $M_w \geq 5.8$ , that have occurred after the last characteristic earthquake of each fault is computed as shown in Figures (2) to (5). Computations are made

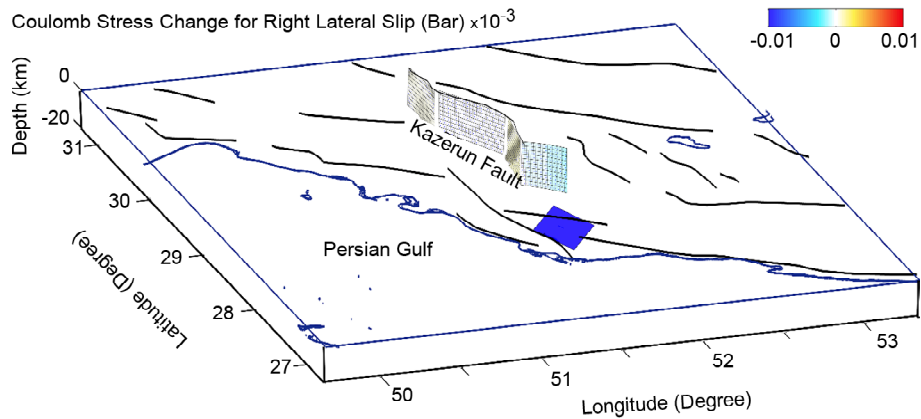
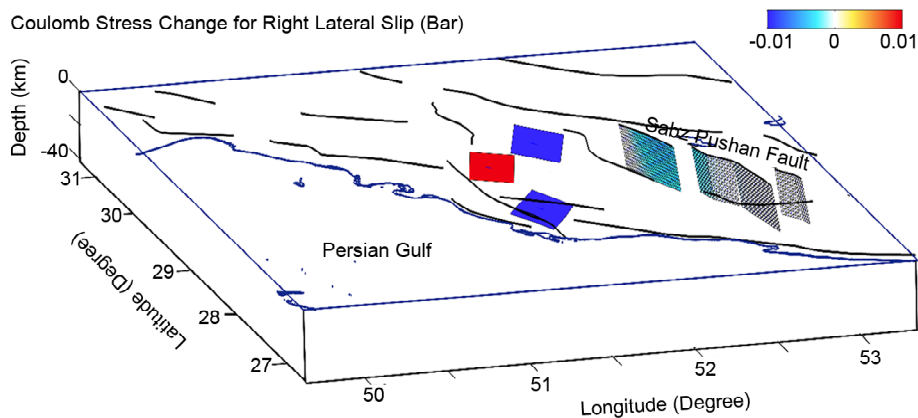
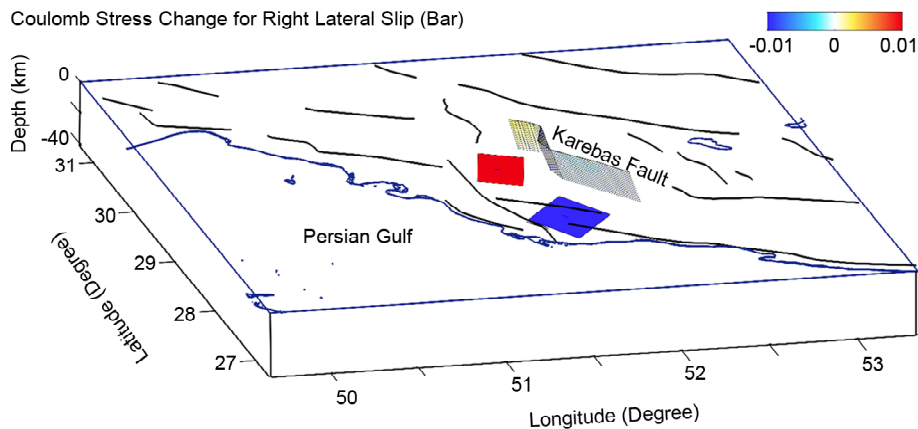


**Figure 2.** Coulomb failure function change ( $\Delta CFF$ ) of Kazerun fault at depth of 10 km caused by relevant earthquakes occurred after 27 September 2010



(a) Sabz Pushan Fault at Depth of 10 km Caused by Relevant Earthquakes Occurred after 20 June 1994



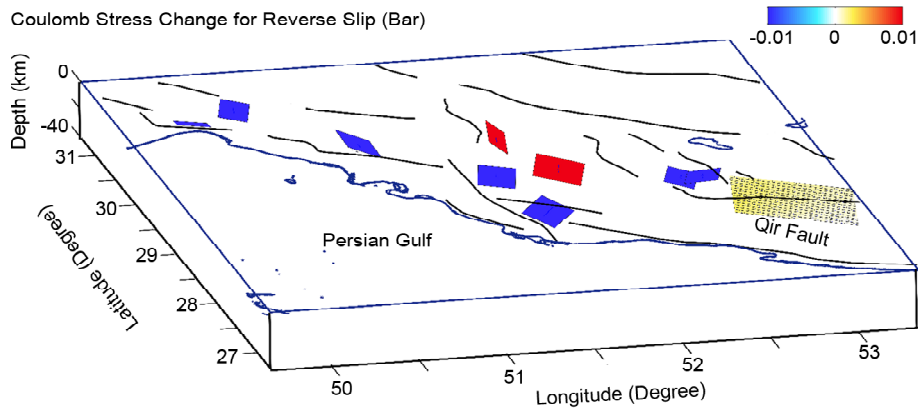
(b) Karebas Fault at Depth of 10 km Caused by Relevant Earthquakes Occurred after 6 May 1999

**Figure 3.** Coulomb failure function change ( $\Delta CFF$ ) of (a) and (b).

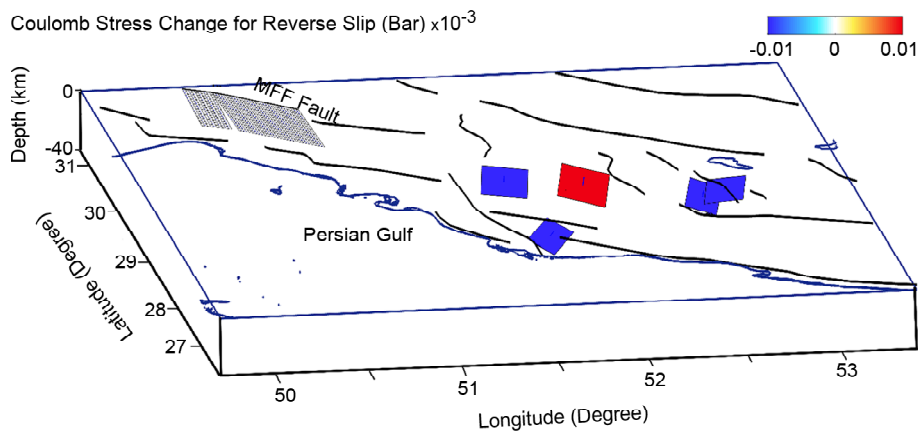
in an elastic halfspace with uniform isotropic elastic properties following Okada [34].

Fault slip rates are the main components of time-dependent seismic hazard studies. Slip rates can be used to estimate activity rates for more sophisticated earthquake models such as the characteristic earthquake model. Khodaverdian et al. [35] modeled the whole area of the Iranian

plateau as a single system of faults (discontinuities) and continuum media using a kinematic finite-element code. They estimated long-term fault slip rates and distributed an elastic strain rates by combining all kinematic data including geological slip rates, geodetic velocities, and stress directions for all over Iran, so that by multiplying the shear modulus by shear strain rate, tectonic strain rates is achieved.



(a) Qir Fault at Depth of 10 km Caused by Relevant Earthquakes Occurred after 10 April 1972



(b) MFF Fault at Depth of 10 km Caused by Relevant Earthquakes Occurred after 10 April 1972

**Figure 4.** Coulomb failure function change ( $\Delta CFF$ ) of (a) and (b).

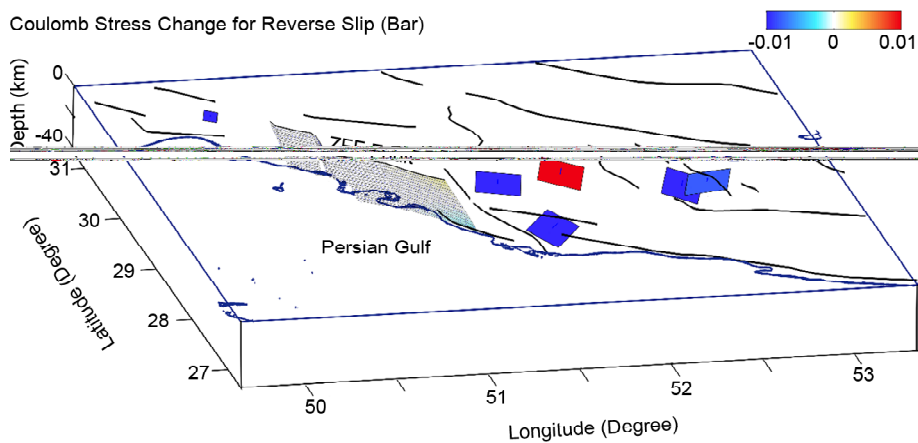


**Figure 5.** Coulomb failure function change ( $\Delta CFF$ ) of ZFF fault at depth of 10 km caused by relevant earthquakes occurred after 27 May 1989.

The historical data of seismic sources presented in this study over a period of time greater than the average return period as well as the paleoseismology data of the seismic sources are not available. Therefore, the annually rate of earthquakes, according to the method described by Fields et al. [36], is determined as follows:

$$Char - Rate = \frac{\dot{M}}{M_0} \tag{12}$$

where  $M_0$  is the moment-magnitude relationship, and  $\dot{M}$  is the moment rate of each segment of fault. The parameter  $M_0$  is expressed based on magnitude  $M$  as:

$$M_0 = 10^{(1.5 * M + C)} \tag{13}$$

where  $C$  is a constant value. The original value of  $C$  was given by Hanks and Kanamori [37] as 9.05 (in SI unit). However, this was apparently rounded off by Anderson and Luco [38] and WGCEP [39] to  $C=9$ . This round off seems apparently innocuous because it results in only 0.075 difference as magnitude is computed from moment (well within the

uncertainties associated with magnitude estimate).

However, using  $C=9$  means that all of magnitudes contain 12.2% less moment than the situation where  $C=9.05$  [37]. Therefore, we set  $C=9.05$ . The moment rate is determined by:

$$\dot{M} = \mu \times V \times L \times W \tag{14}$$

where  $\mu$  is the shear modulus of the elastic medium ( $3.2 \times 10^4$  MPa),  $V$  is the slip rate of fault, and  $L$  and  $W$  are the length and width of a fault with rectangular shape, respectively. Then by inverting the annually rate, we computed the recurrence time of earthquakes in Zagros area. Table (2) lists the required data for the probability computations.

Equation (4) gives the conditional occurrence probability  $P$  in the next 10, 30 and 50 years. If we use  $t'$  instead of  $t$ , the same equation gives the probability modified by the permanent effect of the subsequent earthquakes,  $P_{mod}$ . The probability obtained from the sum of the permanent and the transient effects,  $P_{trans}$ , in the next 10, 30 and 50 years is computed by the Equation (9). Figures (6) to (12) show the results for each of six sources.

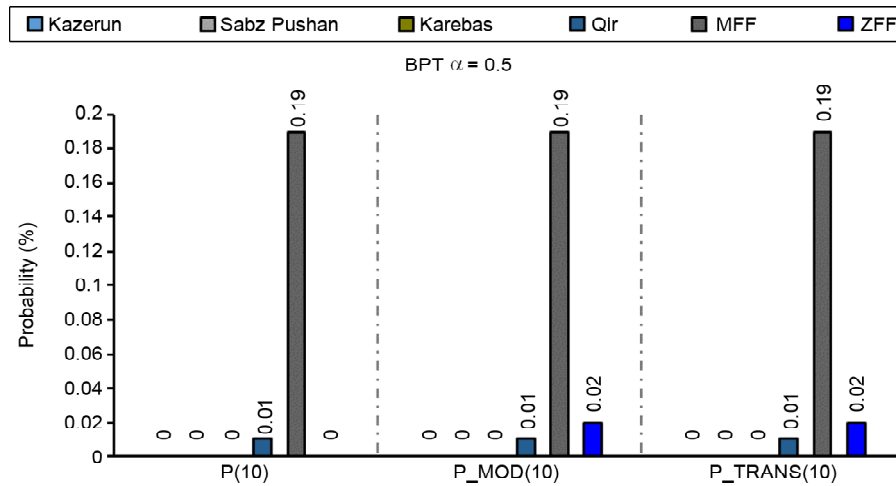


**Figure 6.** Percentage of occurrence probability of a characteristic earthquake on each of six seismogenic faults over 10 years beginning from 2016, according to BPT distribution, using  $\alpha = 0.5$ , by considering permanent and transient effects of stress.

**Table 2.** Computed Coulomb stress change of faults and the parameters used for computing characteristic earthquake occurrence probability in Zagros.

#	Source Name	Strain Rate (Nanostrain/yr)	Tectonic Stressing Rate (pa/yr)	$\Delta\sigma$ (MPa)	Slip Rate (mm/yr)	Slip Rate Uncertainty (mm/yr)	$T_{rmin}/T_{rmax}$	Mean Recurrence Time (yr)	Elapsed Time (yr)	$\Delta\sigma$ (MPa)
1	Kazerun	20.2	646	0.00009	2.48	0.04	111/114	112.4	6	0.0009
2	Sabz Pushan	9.7	312	0.0005	0.8	0.24	268/498	348.4	22	0.0005
3	Karebas	10.9	350	0.002	1.3	0.15	272/343	303.7	17	0.0005
4	Qir	10.7	341	0.0002	2.23	0.31	260/344	296.7	44	0.0005
5	MFF	5.8	185	0.000007	2.44	0.22	130/156	142.1	25	0.0003
6	ZFF	13.4	430	0.001	2.12	0.10	196/215	203.7	27	0.0006

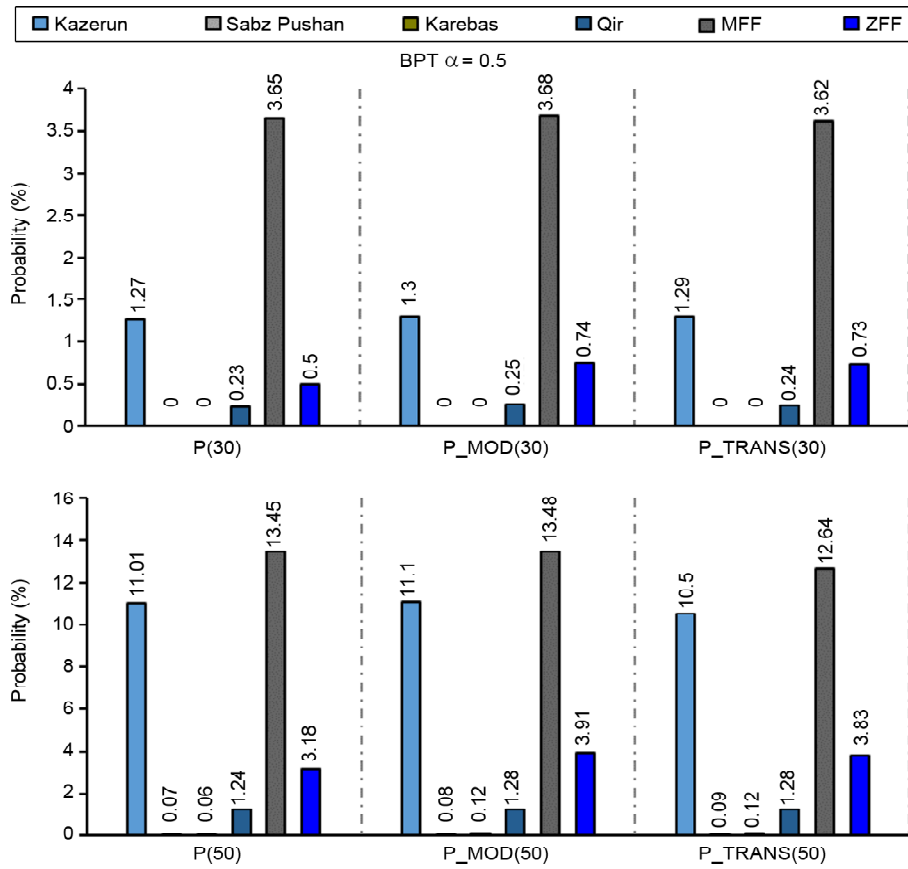


**Figure 7.** Percentage of occurrence probability of a characteristic earthquake on each 6 seismogenic faults over 30 and 50 years beginning from 2016, according to BPT distribution, using  $\alpha = 0.5$ , by considering permanent and transient effects of stress.

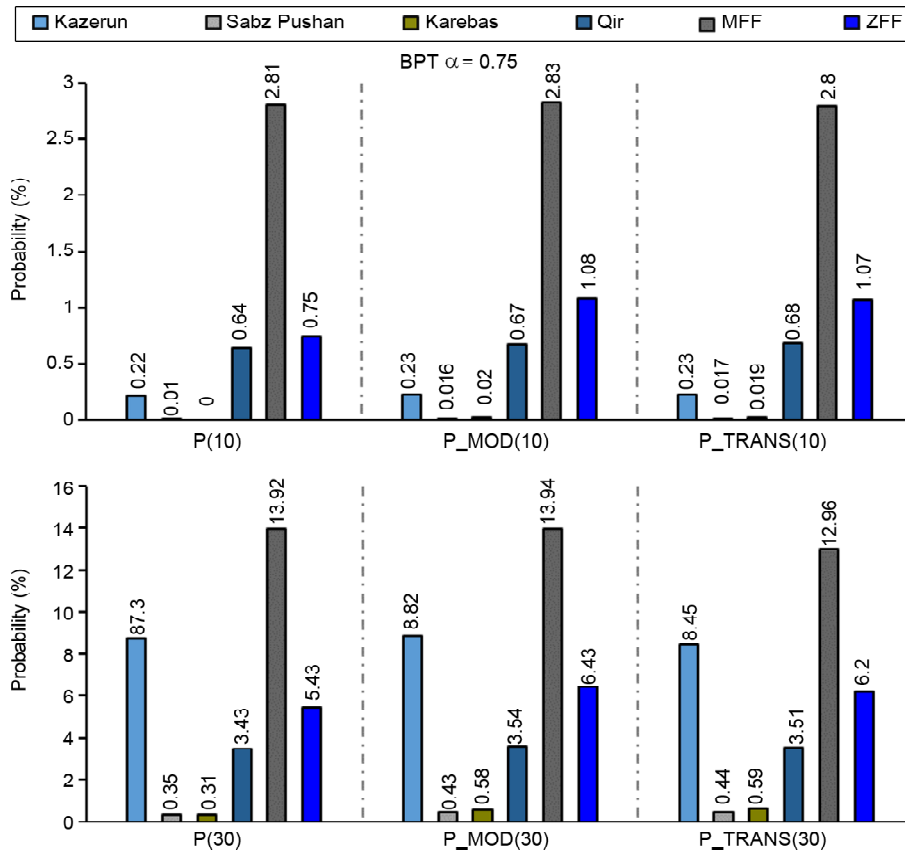
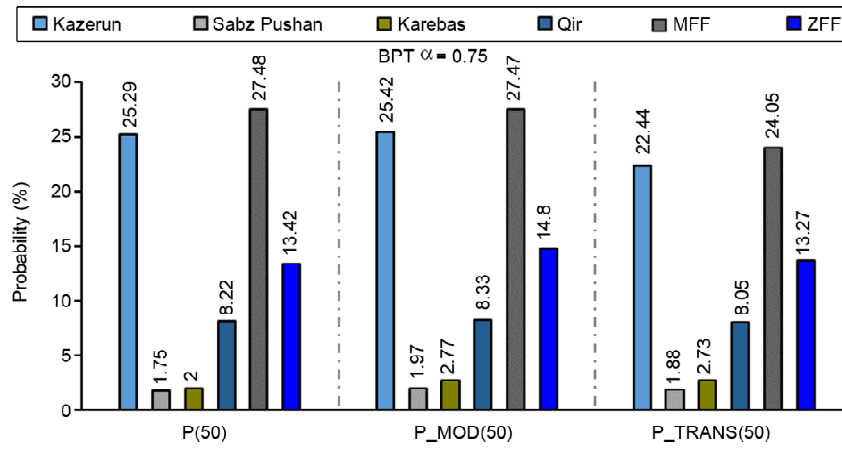
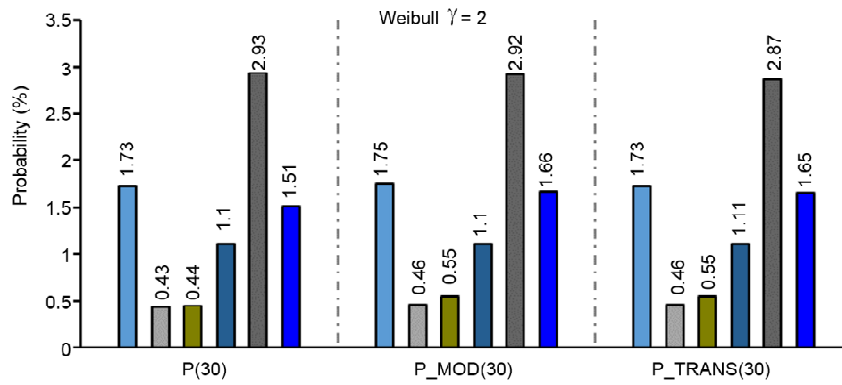


**Figure 8.** Percentage of occurrence probability of a characteristic earthquake on each of six seismogenic faults over 10 and 30 years beginning from 2016, according to BPT distribution, using  $\alpha = 0.75$ , by considering permanent and transient effects of stress..



(a) According to BPT Distribution, Using  $\alpha = 0.75$ , by Considering Permanent and Transient Effects of Stress



(b) According to Weibull Distribution, Using  $\gamma = 2$ , by Considering Permanent and Transient Effects of Stress

**Figure 9.** Percentage of occurrence probability of a characteristic earthquake on each of six seismogenic faults over 50 and 10 years beginning from 2016.

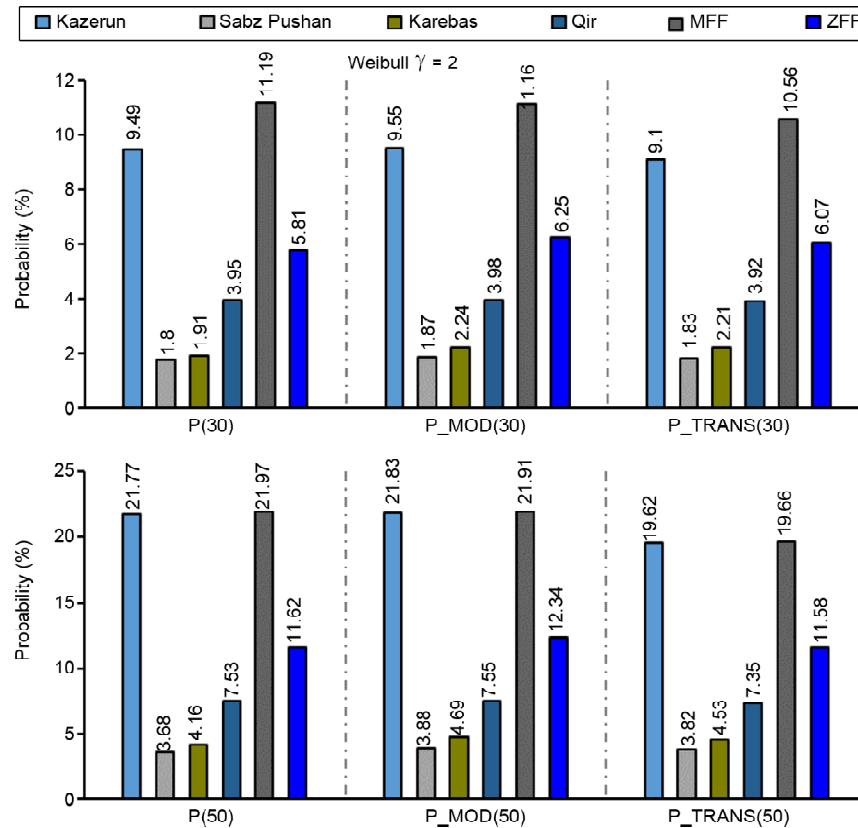


**Figure 10.** Percentage of occurrence probability of a characteristic earthquake on each of six seismogenic faults over 30 and 50 years beginning from 2016, according to Weibull distribution, using  $\gamma = 2$ , by considering permanent and transient effects of stress.

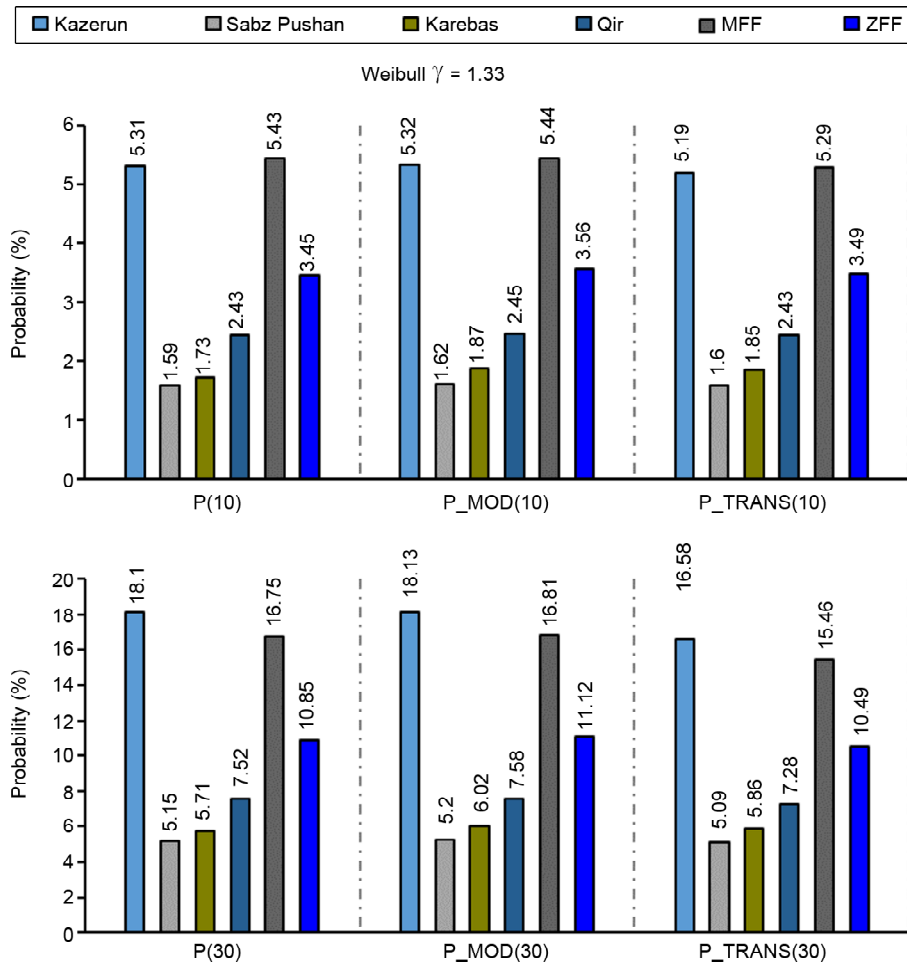


**Figure 11.** Percentage of occurrence probability of a characteristic earthquake on each of six seismogenic faults over 10 and 30 years beginning from 2016, according to Weibull distribution, using  $\gamma = 1.33$ , by considering permanent and transient effects of stress.

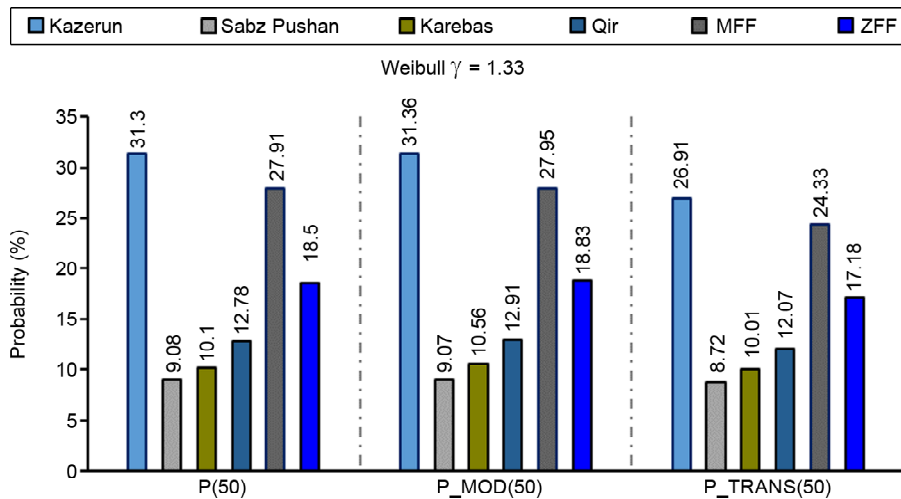


**Figure 12.** Percentage of occurrence probability of a characteristic earthquake on each of six seismogenic faults over 50 year beginning from 2016, according to Weibull distribution, using  $\gamma = 1.33$ , by considering permanent and transient effects of stress.

#### 4. Discussion

Considering the Coulomb stress changes for each fault leads to the following results:

Positive stress change in the western part of the Qir fault plane is more than eastern part. Therefore,

the earthquake occurrence probability would increase in this zone. Slight positive  $\Delta CFF$  of MFF fault (located in the west of Mishan fault) encourages its failure.

In some parts of the ZFF fault (branch connected to the Rag-e Sefid), Coulomb stress change would hasten the rupture. Negative stress created in other parts of the fault causes delay in the failure time. Positive stress is created in the northern part of Karebas fault speeds up the time of the next earthquake. On the contrary, negative stress discourages the rupture time in the southern part.

In most northern parts of the Sabz Pushan fault, where  $\Delta CFF$  is negative, the time of the upcoming large event would delay. In southern part, slightly positive  $\Delta CFF$  is created, which speed up the occurrence time of the next earthquake. Also, because of the orientation of the Kazerun fault plane with respect to the 9 April 2013 earthquake, Coulomb stress changes in parts of the fault close to the location of this earthquake are negative. Vice versa, in parts away from the fault,  $\Delta CFF$  is positive. For all of sources considered in this paper, elapsed time after the last characteristic earthquake is smaller than the mean recurrence time. The calculated probability values with both distributions for ZFF fault are higher than the value calculated for the Sabz Pushan fault. This reflects the fact that with the increase of the gap between elapsed time after the last characteristic event and average return period of the earthquake, the probabilities have smaller values.

The probabilities of earthquake occurrence based on the Weibull distribution for the Karebas fault with regard to permanent effects of Coulomb stress changes ( $P_{mod}$ ) in next 50, 30 and 10 years using  $\gamma = 1.33$  are equal to 10.56%, 6.02% and 1.87%, respectively. This indicates that the probability raises 4.54% in next 50 years compared to the next 30 years. Hence, in a fault zone the probability of an upcoming large event increases with time.

In general, as the mean recurrence time approaches the elapsed time after the last characteristic earthquake, both probabilistic models show high probability values. In a way that: for the Kazerun fault, the probability values computed with both BPT and Weibull models, for all of three models of probability, in most cases are significantly more than the Qir fault. The closeness of elapsed time to average recurrence time in the Kazerun fault with respect to the Qir fault leads to these differences. As, this time difference in the Qir fault is about 2.5 times of the

Kazerun fault.

The probabilities obtained from the permanent effect are mostly higher than the conditional probabilities obtained from the transient effect. This is due to the assumption of constant background rate made for the application of the rate-and-state model, so that the probability in next 50 years for MFF fault based on Weibull model using  $\gamma = 1.33$  including the permanent effects increases 3.24% compared to the probability obtained from the sum of the permanent and the transient effects.

## 5. Conclusions

The present study is an effort to compute the occurrence probability of characteristic earthquakes ( $M_w \geq 5.8$ ) in the region of south west of Iran called Zagros. The methodology applied is based on a model assuming the fault interaction that leads to the triggering of an earthquake by another one. We used renewal models such as BPT and Weibull distribution, including the permanent and transient effect of the stress interaction between six seismogenic sources.

The transient effect of stress change influences on probabilities, so that it causes a slight increase in the amounts of probability in some of sources, while for others the probability is reduced. However, the permanent effects slightly increase the probability values. Our computations showed that earthquake interaction effects in this region are small and range between  $\sim 0.0-0.002$  MPa. Thus, permanent and transient effects of stress change do not affect very much on the calculated probabilities.

The first remarkable result is that for most of the faults both the BPT and Weibull models predicted negligible probability of failure for the next 10, 30 and 50 years, whereas for a few of them both models estimated relatively moderate probability ranging between 20-31 percent. The main reason for these low probability values the short elapsed times, compared with the obtained mean return periods. The recurrence times reported in this study, range from 100-350 years. We deal with the uncertainties in the parameters adopted in the modeling, such as long-term slip rate of faults, magnitude, focal mechanism, recurrence time and coefficient of variation  $\alpha$ . The last two parameters have greatest impact on probability results. The standard

deviation of long term slip rate for faults had a range of about 0.04-0.31 mm/year [35], hence, we concentrated on the long-term slip rate uncertainties through the Monte Carlo technique by generating 1000 random numbers.

It is necessary to note that these values may not be perfectly accurate, because some potential seismic sources might be remained unknown in the Zagros region (i.e., blind faults that have not ruptured yet). High quality and accurate input data for modeling and calculations are of utmost importance that should be considered in order to get more robust results [40-41].

## References

1. Toda, S., Stein, R.S., Richards-Dinger, K., and Bozkurt, S. (2005) Forecasting the evolution of seismicity in southern California: Animations built on earthquake stress transfer. *J. Geophys. Res.*, **110**, doi:10.1029/2004JB003415.
2. Zoller, G. and Hainzl, S. (2007) Recurrence time distributions of large earthquakes in a stochastic model for coupled fault systems: the role of fault interaction. *Bulletin of the Seismological Society of America*, **97**(5), 1679-1687, doi:10.1785/0120060262.
3. Console, R., Falcone, G., Karakostas, V., Murru, M., Papadimitriou, E., and Rhoades, D. (2013) Renewal models and coseismic stress transfer in the Corinth Gulf, Greece, fault system. *Journal of Geophysical Research: Solid Earth*, **118**(7), 3655-3673.
4. Wesnousky, S.G., Scholz, C.H., Shimazaki, K., and Matsuda, T. (1984) Integration of geological and seismological data for the analysis of seismic hazard: A case study of Japan. *Bulletin of the Seismological Society of America*, **74**(2), 687-708.
5. Nishenko, S.P. and Buland, R. (1987) A generic recurrence interval distribution for earthquake forecasting. *Bulletin of the Seismological Society of America*, **77**(4), 1382-1399.
6. Papazachos, B.C. (1992) A time and magnitude predictable model for generation of shallow earthquakes in the Aegean area. *Pure and Applied Geophysics*, **138**(2), 287-308.
7. Boschi, E., Gasperini, P., and Mulargia, F. (1995) Forecasting where larger crustal earthquakes are likely to occur in Italy in the near future. *Bulletin of the Seismological Society of America*, **85**, 1475-1482.
8. The Working Group on California Earthquake Probabilities (1988) *Probabilities of Large Earthquakes Occurring in California on the San Andreas Fault* (USGS Open File Report, Menlo Park, CA), 88-398.
9. Savage, J.C. (1991) Criticism of some forecasts of the national earthquake prediction council. *Bulletin of the Seismological Society of America*, **81**, 862-881.
10. Yadav, R.B.S., Tripathi, J.N., Rastogi, B.K., and Chopra, S. (2008) Probabilistic assessment of earthquake hazard in Gujarat and adjoining region of India. *Pure and Applied Geophysics*, **165**, 1813-1833.
11. Yadav, R.B.S., Tripathi, J.N., Rastogi, B.K., Das, M.C., and Chopra, S. (2010) Probabilistic assessment of earthquake recurrence in north-east India and adjoining regions. *Pure and Applied Geophysics*, **167**, 1331-1342.
12. Matthews, M.V., Ellsworth, W.L., and Reasenber, P.A. (2002) A Brownian model for recurrent earthquakes. *Bulletin of the Seismological Society of America*, **92**(6), 2233-2250.
13. Yakovlev, G., Turcotte, D.L., Rundle, J.B., and Rundle, P.B. (2006) Simulation-based earthquake recurrence times on the San Andreas fault system. *Bulletin of the Seismological Society of America*, **96**(6), 1995-2007.
14. Weibull, W. (1951) A statistical distribution function of wide application. *Journal of Applied Mechanics*, **18**(3), 293-297.
15. Meeker, W.Q. and Escobar, L.A. (1991) *Statistical Methods for Reliability Data using SAS Software*. John Wiley and Sons, New York.
16. Hagiwara, Y. (1974) Probability of earthquake occurrence as obtained from a Weibull distribution analysis of crustal strain. *Tectonophysics*,

- 23, 318-323.
17. King, G.C.P., Stein, R.S., and Lin, J. (1994) Static stress changes and the triggering earthquakes. *Bulletin of the Seismological Society of America*, **84**(3), 935- 953.
  18. Cattin, R., Chamot-Rooke, N., Pubellier, M., Rabaute, A., Delescluse, M., Vigny, C., Fleitout, L., and Dubernet, P. (2009) Stress change and effective friction coefficient along the Sumatra-Andaman-Sagaing fault system after the 26 December 2004 (Mw=9.2) and the 28 March 2005 (Mw = 8.7) earthquakes. *Geochem, Geophys, Geosyst.*, **10**, Q03011.
  19. Harris, R.A. (1998) Introduction to special section: Stress triggers, stress shadows, and implications for seismic hazard. *Journal of Geophysical Research B: Solid Earth*, **103**(10), 24347-24358, doi:10.1029/98JB01576.
  20. Cocco, M. and Rice, J.R. (2002) Pore pressure and poroelasticity effects in Coulomb stress analysis of earthquake interactions. *J. Geophys. Res.*, 107(B2), 2030, doi:10.1029/2000JB000138.
  21. Stein, R., Barka, A., and Dieterich, J. (1997) Progressive failure on the North Anatolian fault since 1939 by earthquake stress triggering. *Geophys. J. Int.*, **128**, 594-604.
  22. Dieterich, J.H. (1994) A constitutive law for rate of earthquake production and its application to earthquake clustering. *J. Geophys. Res.*, **99**, 2601-2618.
  23. Toda, S. and Stein, R.S. (2003) Toggling of seismicity by the 1997 Kagoshima earthquake couplet: A demonstration of time-dependent stress transfer. *J. Geophys. Res.*, **108**, 2567, doi:10.1029/2003JB002527.
  24. Dieterich, J.H. and Kilgore, B. (1996) Implications of fault constitutive properties for earthquake prediction. *Proc. Natl. Acad. Sci.*, **93**(9), 3787-3794.
  25. Gardner, J.K. and Knopoff, L. (1974) Is the sequence of earthquakes in southern California, with aftershocks removed, poissonian? *Bulletin of the Seismological Society of America*, **64**(5), 1363-1367.
  26. Berberian, M., Petrie, C.A., Potts, D.T., Asghari Chaverdi, A., Dusting, A., Sardari Zarchi, A., Weeks, L., Ghassemi, P., and Noruzi, R. (2014) Archaeoseismicity of the mounds and monuments along the Kazerun fault (western Zagros, sw Iranian plateau) since the chalcolithic period. *Iranica Antiqua*, **XLIX**, doi: 10.2143/IA.49.0.3009238.
  27. Baker, C., Jackson, J., and Priestley, K. (1993) Earthquakes on the Kazerun Line in the Zagros Mountains of Iran: strike-slip faulting within a fold and thrust belt. *Geophysical Journal International*, **115**(1), 41-61.
  28. Centroid Moment Tensor catalogue [online]. Available: [www.globalcmt.org/CMTsearch.html](http://www.globalcmt.org/CMTsearch.html) (2016).
  29. Elliott, J.R., Bergman, E.A., Copley, A.C., Ghods, A.R., Nissen, E.K., Oveisi, B., Tatar, M., Walters, R.J., and Yamini-Fard, F. (2015) The 2013 Mw 6.2 Khaki-Shonbe (Iran) Earthquake: insights 1 into seismic and aseismic shortening of the Zagros 2 sedimentary cover. *Earth and Space Science*, **2**, 435-471, doi:10.1002/2015EA000098.
  30. Maggi, A., Jackson, J.A., Priestley, K., and Baker, C. (2000a) A re-assessment of focal depth distributions in southern Iran, the Tien Shan and northern India: do earthquakes really occur in the continental mantle? *Geophysical Journal International*, **143**(3), 629-661.
  31. Talebian, M. and Jackson, J. (2004) A reappraisal of earthquake focal mechanisms and active shortening in the Zagros mountains of Iran. *Geophysical Journal International*, **156**(3), 506-526.
  32. Ni, J. and Barazangi, M. (1986) Seismotectonics of the Zagros continental collision zone and a comparison with the Himalayas. *Journal of Geophysical Research*, **91**(B8), 8205-8218.
  33. Wells, D.L. and Coppersmith, K.J. (1994) New empirical relationships among magnitude, rupture length, rupture width, rupture area, and surface displacement. *Bulletin of the Seismological Society of America*, **84**(28), 974-1002.

34. Okada, Y. (1992) Internal deformation due to shear and tensile faults in a half-space. *Bulletin of the Seismological Society of America*, **82**(2), 1018-1040.
35. Khodaverdian, A., Zafarani, H., and Rahimian, M. (2015) Long term Fault slip rates, distributed deformation rates and forecast of seismicity in the Iranian Plateau. *Tectonics*, **34**(10), 2190-2220.
36. Field, E.H., Johnson, D.D., and Dolan, J.F. (1999) A mutually consistent seismic-hazard source model for Southern California. *Bulletin of the Seismological Society of America*, **89**(3), 559-578.
37. Hanks, T.C. and Kanamori, H. (1979) A moment magnitude scale. *J. Geophys. Res.*, **84**, 2348-2350.
38. Anderson, J.G. and Luco, J.E. (1983) Consequences of slip rate constraints on earthquake occurrence relations. *Bulletin of Seismological Society of America*, **73**, 471-496.
39. Working Group on California earthquake probabilities (1995) Seismic hazard in southern California: probable earthquakes, 1994 to 2024. *Bulletin of the Seismological Society of America*, **85**, 379-439.
40. Jalalhosseini, S.M., Zafarani, H., and Zare, M. (2018) Time-dependent seismic hazard analysis for the Greater Tehran and surrounding areas. *Journal of Seismology*, **22**, 187-215.
41. Akinci, A., Murru, M., Consol, R., Falcone, G., and Pussi, S. (2014) Implications of earthquake recurrence models to the seismic hazard estimates in the Marmara region, Turkey. *Second European Conference on Earthquake Engineering and Seismology*, Istanbul.